From Caledonian Collapse to North Sea Rift: The Extended History of a Metamorphic Core Complex

J. D. Wiest[1] [ID], T. Wrona[2] [ID], M. S. Bauck[3,4], H. Fossen[1,5] [ID], R. L. Gawthorpe[1] [ID], P. T. Osmundsen[4,6] [ID], and J. I. Faleide[4]

[1]Department of Earth Science, University of Bergen, Bergen, Norway, [2]GFZ German Research Centre for Geosciences, Potsdam, Germany, [3]CGG, Oslo, Norway, [4]Department of Geosciences, University of Oslo, Oslo, Norway, [5]Department of Natural History, University Museum of Bergen, Bergen, Norway, [6]Department of Geoscience and Petroleum, Norwegian University of Science and Technology (NTNU), Trondheim, Norway

Abstract Extensional systems evolve through different stages due to changes in the rheological state of the lithosphere. It is crucial to distinguish ductile structures formed before and during rifting, as both cases have important but contrasting bearings on the structural evolution. To address this issue, we present the illustrative ductile-to-brittle structural history of a metamorphic core complex (MCC) onshore and offshore western Norway. Combining geological field mapping with newly acquired 3-D seismic reflection data, we correlate two distinct onshore basement units (BU1 and BU2) to corresponding offshore basement seismic facies (SF1 and SF2). Our interpretation reveals two 40 km wide domes (one onshore and one offshore), which both show characteristic kilometer-scale, westward plunging upright folds. The gneiss domes fill antiformal culminations in the footwall of a >100 km long, shallowly west dipping, extensional detachment. Overlying Caledonian nappes and Devonian supradetachment basins occupy saddles of the hyperbolic detachment surface. Devonian collapse of the Caledonian orogen formed dome and detachment geometries. During North Sea rifting, brittle reactivation of the MCC resulted in complex fault patterns deviating from N-S strike dominant at the eastern margin of the rift. Around 61°N, only minor N-S faults (<100 m throw) cut through the core of the MCC. Major rift faults (≤5 km throw), on the other hand, reactivated the detachment and follow the steep flanks of the MCC. This highlights that inherited ductile structures can locally alter the orientation of brittle faults formed during rifting.

Plain Language Summary The mechanical behavior of the lithosphere largely determines the style of crustal deformation. Therefore, many areas go successively through different modes of extension. In the case of a thick and warm crust, extension can form ductile domes below low-angle normal faults, so-called metamorphic core complexes (MCCs). Onshore West Norway, we observe a MCC formed during Devonian collapse of the Caledonian orogen. Offshore, new 3-D seismic data reveal a second dome underneath rift basins in the northern North Sea. Both domes are connected through a 100 km long extensional high strain zone, which formed during Caledonian collapse. The combination of ductile and brittle processes formed a deformation zone with nonplanar geometry, which consists of a series of domes and saddles. About 140 Myr later, Permian-Triassic rifting formed large normal faults, which exploited the inherited weakness of the deformation zone. This brittle reactivation resulted in strongly deviating rift fault orientations around 61°N.

1. Introduction

The rheological state of the lithosphere largely determines the mode of continental extension (Brun et al., 2018; Brune et al., 2017; Buck, 1991; Whitney et al., 2013). From orogen collapse to continental breakup, extensional systems evolve through distinct stages with fundamentally different structural styles (Peron-Pinvidic et al., 2013). Recent 2-D seismic surveys of passive margins revealed the important influence of ductile flow in the lower crust on contrasting time-temperature-deformation histories (Clerc et al., 2018; Jolivet et al., 2018; Osmundsen & Péron-Pinvidic, 2018). Due to the superposition of progressive extensional phases, however, it can be challenging to reconstruct the relation of variably ductile and brittle structures during different stages of margin evolution. Failed rifts that never reached the coupling stage, on the
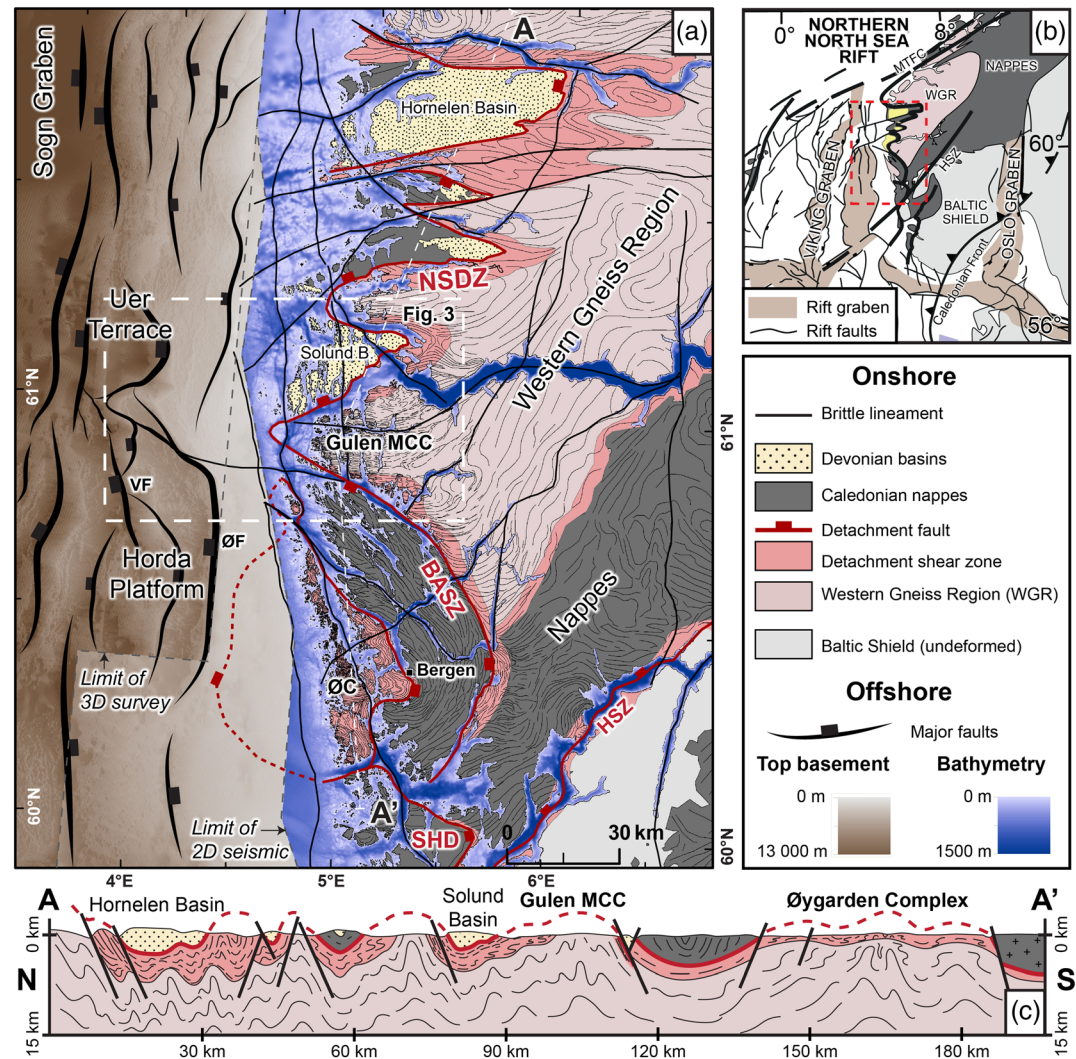
Figure 1. (a) Onshore-offshore map of West Norway and the northern North Sea. The offshore map shows the surface of the prerift basement and major faults. Bathymetry fills the gap between seismic coverage and onshore units formed during the Caledonian orogeny and Devonian collapse. The Gulen MCC and the Øygarden Complex (ØC) represent the onshore analogues of this study. (b) Location of the study area in the North Sea rift (modified from Fossen et al., 2016). (c) Regional N-S cross section along the strike of the undulating detachment, modified from Wiest et al. (2020). Abbreviations: BASZ = Bergen Arcs shear zone; HSZ = Hardangerfjord shear zone; MTFC = Møre-Trøndelag fault complex; NSDZ = Nordfjord-Sogn detachment zone; SHD = Sunnhordland detachment; VF = Vette Fault; ØF = Øygarden Fault.

other hand, can provide important insights for the influence of structural inheritance on early rift phases (Fazlikhani et al., 2017; Fossen et al., 2016; Phillips et al., 2019).

Both field and seismic studies have strengths and weaknesses when it comes to the study of ductile and brittle structures. In the field, we can directly determine rock types, date absolute ages, and constrain conditions, kinematics, and mechanisms of deformation. Field observations, however, are restricted to surface exposures. State-of-the-art 3-D seismic reflection data, on the other hand, reveal three-dimensional structural geometries over large areas and to great depths. Since both methods complement each other, this study combines onshore and offshore observations to address the progressive evolution of a metamorphic core complex (MCC) from orogen collapse to rifting. At the west coast of Norway, Wiest et al. (2019) mapped the Gulen MCC that formed during collapse of the Caledonides (Figure 1). Directly offshore, the eastern margin of the northern North Sea is marked by high structural complexity around 61°N and represents an

important boundary between distinct rift domains (Horda Platform (south)-Uer Terrace (north); Figure 1) (Bell et al., 2014; Færseth et al., 1995; Fazlikhani et al., 2017; Fossen et al., 2016; Lenhart et al., 2019). Newly acquired Broadband 3-D seismic reflection data give an unprecedented image of deep structures in the northern North Sea and allow for correlation of onshore basement units with 3-D seismic facies offshore. The onshore-offshore correlation allows us to investigate (1) three-dimensional aspects of dome and detachment formation and (2) the role of the inherited MCC during rifting.

2. Geological Setting

The study area (Figure 1) represents the transition from 30 km thick continental crust onshore West Norway into the northern North Sea rift, where crystalline basement is overlain by up to 12 km of synrift and postrift sedimentary strata (Christiansson et al., 2000; Maystrenko et al., 2017; Stratford et al., 2009). Onshore, the crystalline basement consists of four main units: Variably reworked Baltic Shield, Caledonian allochthons, extensional detachment zones, and Devonian supradetachment basins. The continental crust of the Baltic Shield formed before and during the ~1.0 Ga Sveconorwegian orogeny (Bingen et al., 2005; Roberts & Slagstad, 2015; Slagstad et al., 2013) and contains mafic bodies included in granitic rocks (Wiest et al., 2018). During the Silurian to Early Devonian Caledonian orogeny (Gee et al., 2008), the Baltican margin was subducted below Laurentia, while nappes of oceanic and continental origin were imbricated and thrust onto the Baltic Shield toward the SE (Corfu et al., 2014; Fossen et al., 2017). The "Caledonized" part of the Baltican margin in the Western Gneiss Region (WGR) records gradually increasing metamorphic conditions (e.g., Cuthbert et al., 2000; Griffin & Brueckner, 1980) and deformation intensity from SE to NW (Hacker et al., 2010; Milnes et al., 1997). During Devonian postcollisional collapse of the Caledonian orogen (Fossen, 2000, 2010), the deeply buried thermally softened crust was subject to pervasive ductile flow (Gordon et al., 2013; Labrousse et al., 2004). Boundary conditions of sinistral transtension imposed a constrictional strain regime, while metamorphic variations resulted in contrasting deformation styles at distinct crustal levels (Andersen et al., 1994; Fossen et al., 2013; Krabbendam & Dewey, 1998; Osmundsen & Andersen, 2001; Wiest et al., 2019). Strongly undulating detachments exhumed MCCs with extension-parallel gneiss/migmatite domes (Figure 1c) along the west coast of Norway (Braathen et al., 2000; Johnston et al., 2007; Labrousse et al., 2002; Norton, 1986; Osmundsen et al., 2005; Wiest et al., 2020). Detachment shearing evolved progressively from amphibolite facies to brittle conditions (Braathen et al., 2004) and variably overprinted upper parts of the WGR (Andersen et al., 1994; Wennberg et al., 1998), lower parts of the orogenic wedge (Hacker et al., 2003; Osmundsen & Andersen, 1994) and the base of scoop-shaped Devonian supradetachment basins (Séguret et al., 1989; Seranne & Seguret, 1987; Vetti & Fossen, 2012). Later on, multiple phases of brittle extension reactivated the Devonian structures (Andersen et al., 1999; Eide et al., 1997; Fossen et al., 2016; Ksienzyk et al., 2016; Larsen et al., 2003; Torsvik et al., 1992).

A first phase of North Sea rifting in the Late Permian to Early Triassic lasted for around 30 Myr (Ter Voorde et al., 2000; Ziegler, 1982). E-W directed rifting affected a wide area and was strongly controlled by inherited structural heterogeneities (Christiansson et al., 2000; Fazlikhani et al., 2017; Phillips et al., 2019). On the Horda Platform (Figure 1a), rifting resulted in the development of major half-grabens bound by west dipping normal faults (Whipp et al., 2014). A second phase of Middle Jurassic to Early Cretaceous rifting (Bell et al., 2014; Færseth et al., 1997) comprised diachronous fault activity (~10–40 Myr) across the rift (Claringbould et al., 2017; Cowie et al., 2005). The extension direction of this second rift phase is debated in between E-W (Bartholomew et al., 1993) and NW-SE (Doré et al., 1997; Færseth et al., 1997). In contrast to the first rift phase, fault activity became strongly localized in the Viking and Sogn grabens while only minor fault reactivation affected the eastern rift shoulder on the Horda Platform (Phillips et al., 2019). In the following, active extension shifted northward related to opening of the North Atlantic and the northern North Sea experienced a period of postrift thermal subsidence (Odinsen et al., 2000).

3. Data and Methods

3.1. Field Observations

The description of the Gulen MCC by Wiest et al. (2019) provides the onshore part of this study, complemented by observations from the detachment footwall exposed in the Øygarden Complex (Wiest et al., 2018,
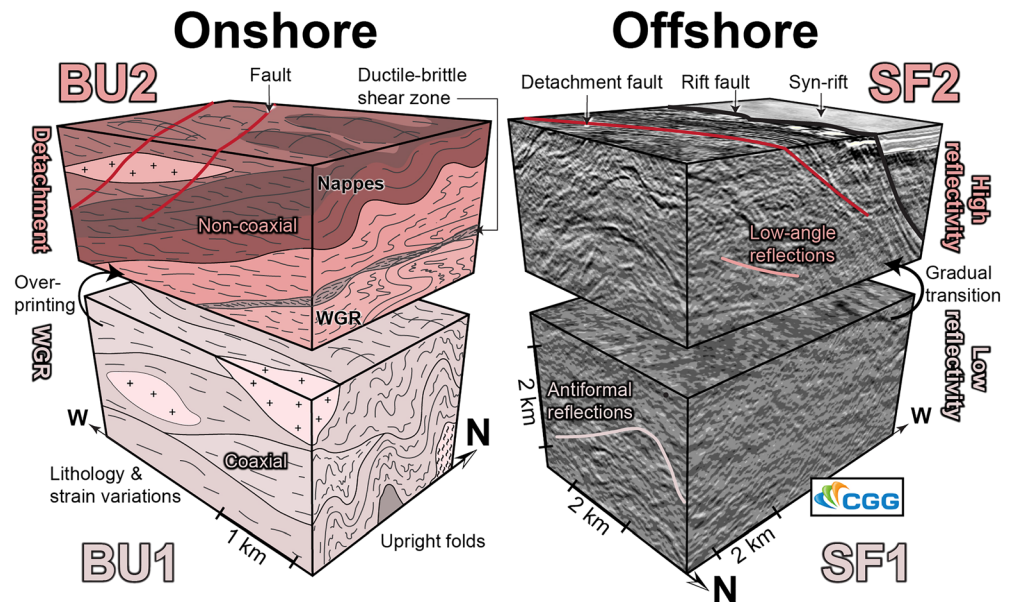
Figure 2. Schematic illustration showing characteristics of onshore basement units (BU, left) suggested for correlation with 3-D seismic facies (SF, right). The seismic cubes have a vertical exaggeration of 1.5 and are shown in perspective view from NE. Note the gradual transition between the seismic facies and overprinting of the Western Gneiss Region (WGR; BU1) by the detachment (BU2). Seismic data courtesy of CGG.

2020). The Gulen MCC is a westward plunging antiform consisting of a high-grade metamorphic core with subvertical foliations flanked by detachment shear zones (Figure 1). The structure is asymmetric with a shallow N-NW dipping flank and a steep S-SW dipping flank. Next to the dome, Caledonian allochthons and Devonian supradetachment basins occupy synforms in the hanging wall of the detachment. The core of the Gulen dome formed through extension-perpendicular flow of low-viscosity (solid-state) material in deep crustal channels in response to upper crustal thinning (Wiest et al., 2019). Detachment shearing involved noncoaxial deformation, vertical shortening, and retrogressive phyllosilicate growth leading to fabric weakening (Wiest et al., 2020). We summarize the main characteristics of the two distinct basement units that define the Gulen MCC.

3.1.1. Basement Unit 1 (BU1): WGR

The WGR in the antiformal core of the dome (Figures 2 and 3) consists of Proterozoic crust that was pervasively migmatized and intruded by granites during the Sveconorwegian orogeny (Røhr et al., 2004; Wiest et al., 2019). Isolated layers of quartzites and schists are preserved within the migmatites. Mafic bodies range in size from a few meters to ~20 km and were variably converted to eclogites during the Caledonian orogeny. Ductile deformation during postorogenic collapse involved simultaneous coaxial E-W stretching and N-S shortening. A network of shear zones formed in the eastern part of the complex that merge toward the west into pervasively deformed mylonites (Figure 3a). The resulting gneissic tectonites (Figure 2) have a strong fabric anisotropy with subhorizontal E-W trending lineations and parallelly striking subvertical foliations. The gneissic foliations are folded into upright folds, which occur from the centimeter to the kilometer scale (Figure 3c). Homogeneous granites and mafic bodies form meter- to kilometer-scale low-strain domains in the pervasively deformed gneisses (Figure 3d).

3.1.2. Basement Unit 2 (BU2): Detachment Zone

Detachment mylonites are characterized by asymmetric fabrics related to noncoaxial shearing and shallowly dipping foliations related to vertical shortening (Figure 2). Retrograde fluid-induced phyllonitization localized strain in ductile-to-brittle shear zones in the lower, WGR-derived detachment mylonites (Wiest et al., 2020). Large parts of the detachment zones, however, are nappe-derived and comprise dominantly schists besides other heterogeneous lithologies. The schists of the Hyllestad complex, for example, contain the Sogneskollen granite as a 3 km wide, low-strain lens (Hacker et al., 2003). Brittle faulting becomes more and more prominent toward the contact with the Devonian basins (Braathen et al., 2004), although parts of the lowermost Devonian strata have been ductilely deformed (Seranne & Seguret, 1987). The combination of
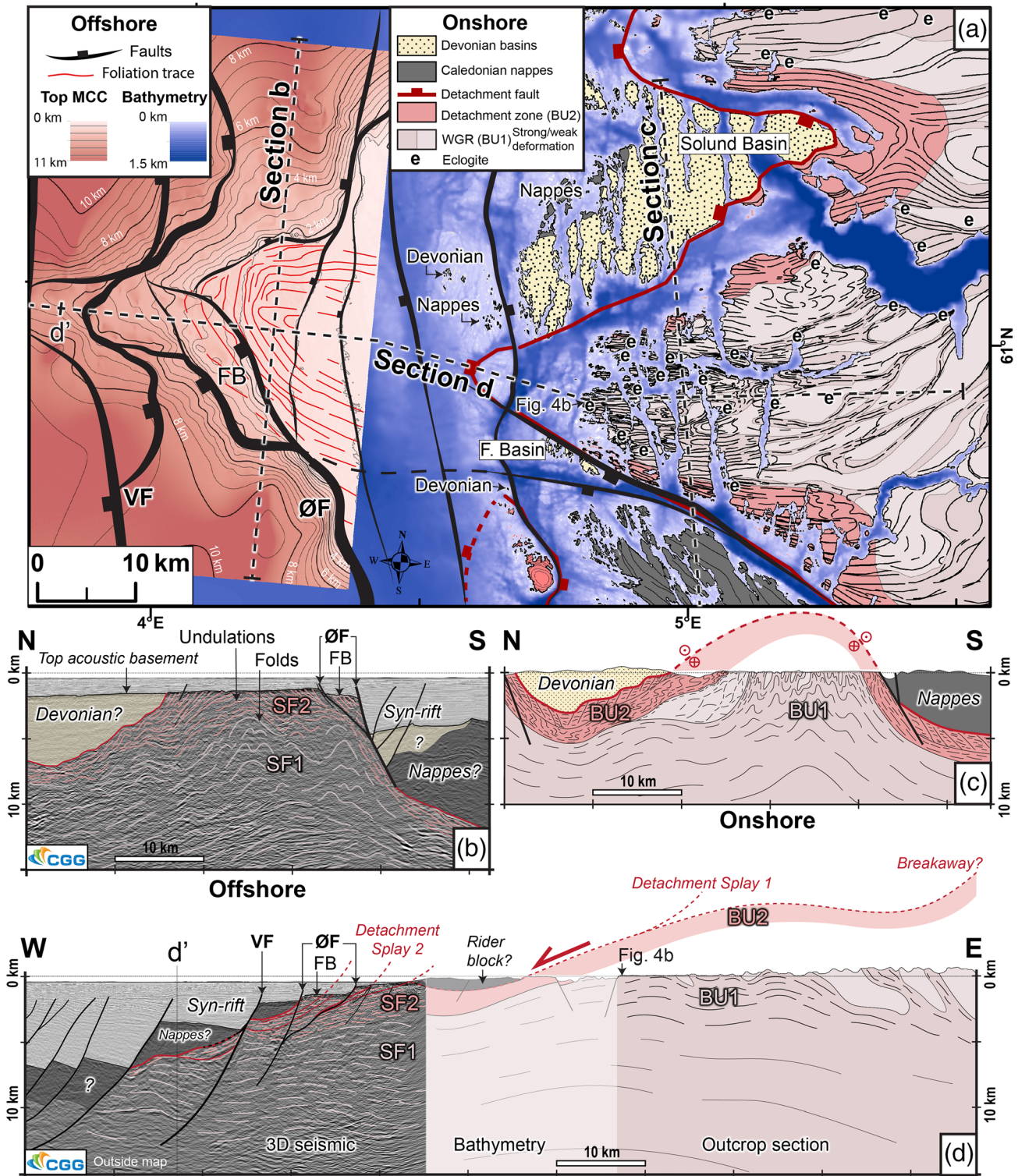
Figure 3. Onshore-offshore map and cross sections of the study area; onshore parts modified from Wiest et al. (2019). (a) The offshore map shows the depth-contoured enveloping surface of the MCC. Foliation traces are interpreted from amplitude variance patterns on the top acoustic basement erosion surface. Similar to the Fensfjorden basin onshore, a fault-bound block rests on the steep SW flank of the offshore dome (marked as FB). (b and c) N-S cross sections of the offshore (b) and onshore domes (c). A rift fault associated with ~5 km synrift fill reactivated the steep southern flank of the offshore dome. (d) Extension-parallel E-W cross section showing our onshore-offshore interpretation of the detachment zone. All cross sections are drawn with 1.5 vertical exaggeration. VF = Vette Fault; ØF = Øygarden Fault. Seismic data courtesy of CGG.

Figure 4. Outcrop-scale field examples showing variable relationship between brittle faults and ductile structures described by Wiest et al. (2019) and Wiest et al. (2020). (a) Steeply dipping foliation surface reactivated as fault plane coated with chlorite and epidote. BU1, Gulen MCC. (b) Steep fault in biotite-rich layer at the steep limb of tight upright folds in gneiss. BU1, Gulen MCC. (c) Subhorizontal fault gouge localized in garnet-mica schis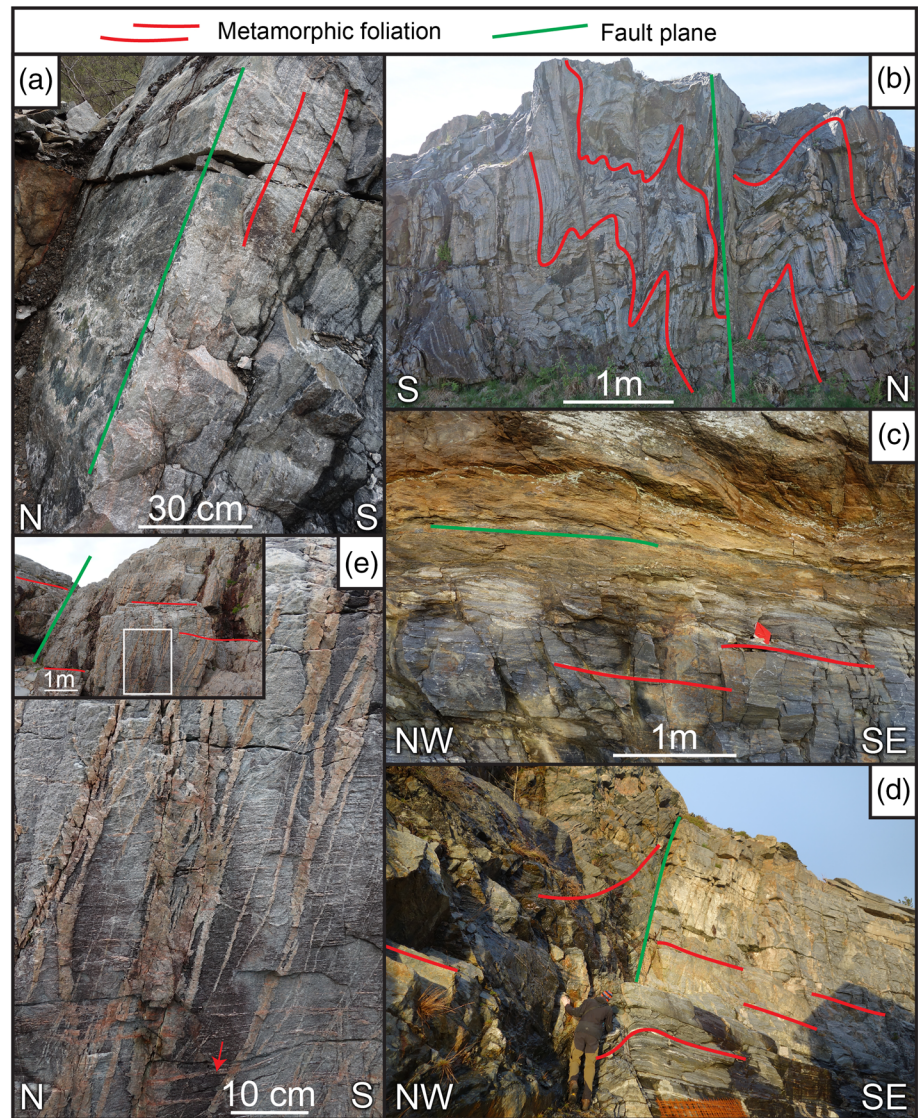t. BU2, Øygarden Complex. (d) Steep fault cross-cutting subhorizontal phyllonitic shear zone. Note the drag of the foliation. BU2, Øygarden Complex. (e) Feldspar alteration (orange) in the damage zone of a steep fault in gray gneiss (inset shows overview). Most of the alteration zones follow steep fractures, which run parallel to the fault, but some follow the subhorizontal metamorphic foliation (red arrow). BU2, Øygarden Complex.

ductile and brittle deformation has juxtaposed rocks from the former orogenic root with sediments deposited during collapse. Today, we find eclogites within the Gulen dome only 3 km away from the Fensfjorden basin (Figure 3a).

3.1.3. Brittle Reactivation of Ductile Structures

Both, the Gulen dome and the Øygarden Complex, have abundant exposures (Figure 4) that show a variable relationship of Early Devonian to Mesozoic brittle faults (Fossen et al., 2016; Ksienzyk et al., 2014, 2016; Larsen et al., 2003) and ductile structures mostly formed during Caledonian postorogenic collapse (Wiest et al., 2019, 2020). Steep foliation surfaces have been commonly reactivated as brittle slip surfaces (Figure 4a), especially where mica-rich layers are present (Figure 4b). Many low-angle shear zones in the detachment domain contain phyllonitic layers. Sometimes, these weak layers have been reactivated as subhorizontal brittle faults (Figure 4c), but more commonly, they are cut at a high angle by steep faults

(Figure 4d). Feldspar alteration zones in granitic gneiss (see also Fossen et al., 2016) run along preexisting foliation planes and cross-cutting fractures (Figure 4e) and exemplify the highly variable influence of preexisting fabrics, even on a small scale.

3.2. Three-Dimensional Seismic Reflection Data

We use recently acquired broadband 3-D seismic reflection data (courtesy of CGG) of the northern North Sea rift (Figure 1) imaging down to depths of 22 km. The data were acquired using a series of up to 8 km long streamers towed ~40 m deep. Data recording extends to 9 s with a time sampling of 4 ms. BroadSeis data cover a wide range of frequencies reaching from 2.5 to 155 Hz. The data were binned at 12.5×18.75 m. The data set was 3-D true amplitude Kirchhoff prestack depth migrated. The seismic data was zero-phase processed with SEG normal polarity; that is, a positive reflection (white) corresponds to an acoustic-impedance increase with depth.

Our seismic interpretation (supporting information Figure S1) is based on a 3-D facies analysis of the acoustic basement, which includes units beneath the Permian-Triassic strata, including Devonian (meta)sediments, Caledonian, and pre-Caledonian crystalline rocks. Since the basement units are neither penetrated by wells nor separated by coherent reflectors, the subdivision into seismic facies is based on their appearance in 3-D and builds upon previous work by Fazlikhani et al. (2017) and Lenhart et al. (2019).

4. Basement Seismic Facies Observed Offshore

The 3-D seismic data clearly show the top acoustic basement surface as a continuous, high-amplitude reflection originating from the impedance contrast between synrift/postrift sedimentary rocks above and basement rocks below. Our study focuses on the identification of two seismic facies (Figure 2), which define a domal structure in the acoustic basement (Figure 3 and supporting information Figure S1). Other basement units are marked tentatively to highlight structural geometries in our interpretation but are not subject of this study.

4.1. Seismic Facies 1 (SF1): WGR

Seismic Facies 1 (SF1) occurs at the lower levels of our sections and comprises up to 90% of the imaged basement in terms of thickness (up to 20 km). In both N-S and E-W direction, SF1 appears as chaotic low-to-medium amplitude reflections with isolated patches of high amplitudes (Figure 2). Below 10–12 km depth, reflectivity increases and defines a pattern consisting of subhorizontal reflections, which are sometimes parallel and sometimes crisscrossing and terminating against each other in E-W sections (Figure 3d). In N-S sections, reflections dip in opposite directions at ~25° and define upright folds commonly with wavelengths of several kilometers (Figure 3b).

4.2. Seismic Facies 2 (SF2): Detachment Zone

The transition from SF1 to SF2 occurs gradually over a thickness of 1–3 km and coincides with an upward increase in reflectivity provided by shallowly west dipping reflections that undulate in N-S sections with wavelengths from hundreds of meters to several kilometers (Figures 2 and 3b). The upper part of SF2 is characterized by closely (<300 m) spaced swarms of shallowly west dipping, medium-to-high amplitude reflections, which partly cross cut and partly sole out in subhorizontal reflections. These medium-to-high amplitude reflections steepen from ~10° at the base up to ~30° at the top where they are truncated by the top acoustic basement erosion surface. We interpret these reflections as brittle detachment faults formed during postorogenic collapse (Fossen et al., 2016). Besides the top acoustic basement surface, the top of SF2 is marked by a transition into undifferentiated basement lacking the characteristic reflections of SF2. SF2 is highly variable in thickness, reaching up to 4 km in the east, while locally disappearing toward the west (Figure 3d).

5. Interpretation

In this section, we highlight similarities and differences between basement units mapped onshore and seismic facies observed in offshore seismic reflection data. The onshore-offshore correlation allows us to produce a unified geological interpretation.

5.1. Correlation Between Basement Units (Onshore) and Seismic Facies (Offshore)

One similarity between basements units and seismic facies is the sequence, depth, and thickness at which they occur. Basement Unit 1 and SF1 both occur at the deepest level, while BU2 and SF2 are overlying. SF2 is of laterally variable thickness, which is also the case for BU2. In N-S direction, antiformal reflections are observed in both seismic facies with decreasing fold amplitude from SF1 to SF2 (Figure 3). Correspondingly, the gneisses in the core of the onshore dome (BU1) are pervasively upright folded, while vertical shortening formed recumbent folds superposed on kilometer-scale upright undulations in the detachment zone (BU2). The transition from SF1 to SF2 is gradual and similarly, the transition from BU1 to BU2 involves the gradual overprinting of WGR gneisses in the detachment zone. In general, both basement units consist of similar rock types, but the larger lithological and structural heterogeneity of the detachment zone (BU2) compared to the WGR (BU1) may explain the generally higher reflectivity of SF1 compared to SF2. For instance, BU1 consists of rocks with a strong fabric anisotropy besides strain-related and compositional variations (e.g., different magmatic protoliths). Nevertheless, they are unlikely to translate into high amplitude seismic reflections given that they often are (1) dipping vertically, (2) at or below the seismic resolution, (3) without large impedance contrasts, (4) gradual, rather than discrete, and (5) homogenized by pervasive deformation. As such, it is plausible to correlate BU1 with SF1, a chaotic, incoherent seismic facies, which only occasionally shows isolated patches of high amplitudes. The contrasting reflection characteristics and geometries correlate SF2 to Devonian extensional shear zones (BU2) (Fazlikhani et al., 2017; Lenhart et al., 2019; Phillips et al., 2016). The retrograde development of ductile-to-brittle shear zones through fluid-induced weakening in the detachment zone (Braathen et al., 2004; Wiest et al., 2018, 2020) can explain the occurrence of shallow-dipping, high-amplitude reflections at the base of SF2 (Figure 2). Low-angle brittle faults in the upper part of the detachment zone can explain the abundance of moderately inclined, planar seismic reflections toward the top of SF2.

5.2. Three-Dimensional Structural Geometries From Onshore to Offshore

Our 3-D seismic interpretation constrains an offshore dome in direct continuation west of the Gulen dome (Figure 3). The offshore map shows the morphology of the enveloping surface of the dome observed in the seismic data (Figure 3a). This surface is a combined product of faulting and erosion reshaping a previously ductile structure (supporting information Figure S2). The latter is recognized in folded foliation traces, which have been interpreted from amplitude variance patterns on the top acoustic basement erosion surface. The >100 km long E-W section (Figure 3d) connects onshore and offshore observations and shows rift faults with displacements increasing from tens of meters in the coastal areas to ≥5 km in the west. Exposures on scattered islands (Figure 3a) and bathymetry help to bridge a 20 km gap along the E-W section between the 3-D seismic survey and coastal exposures.

5.2.1. Dome Geometries

Extension-perpendicular N-S sections through the offshore (Figure 3b) and onshore domes (Figure 3c) highlight several key observations. (1) Erosion has exposed different levels of the MCCs; onshore the core of the dome (BU1) and offshore the detachment (SF2). (2) The detachment offshore connects both flanks of the dome. (3) Synformal units next to the offshore dome can be correlated to Devonian basin fill to the north and Caledonian allochthons to the south of the onshore dome. (4) Both domes show upright folds of kilometer-scale wavelengths and amplitudes, the latter of which decrease in the detachment zone. (5) Both domes are asymmetric with shallow northern and steep southern flanks. (6) The steep southern flank offshore was reactivated by the Øygarden Fault accommodating ~5 km of synrift strata. At the same latitude, the shallow northern flank shows little fault activity. (7) The Fensfjorden Devonian basin is found in a fault-bound block at the SW flank of the onshore dome (Figure 3a). Similarly, two splays of the Øygarden Fault enclose a 20 km × 4 km block (marked with FB) with characteristics of SF2 on the SW flank of the offshore dome.

5.2.2. Detachment Zone Geometry

Connecting the onshore outcrops of the detachment to the offshore interpretation of SF2 (Figure 3d) requires either an east dipping normal fault with several kilometers throw, or alternatively, bends of the detachment surface in E-W direction. Since fault displacements decrease toward the eastern part of the seismic section and such large displacements are not observed in near-coastal areas, we prefer a coherent detachment zone in our interpretation. This is also in agreement with the occurrence of upper plate units
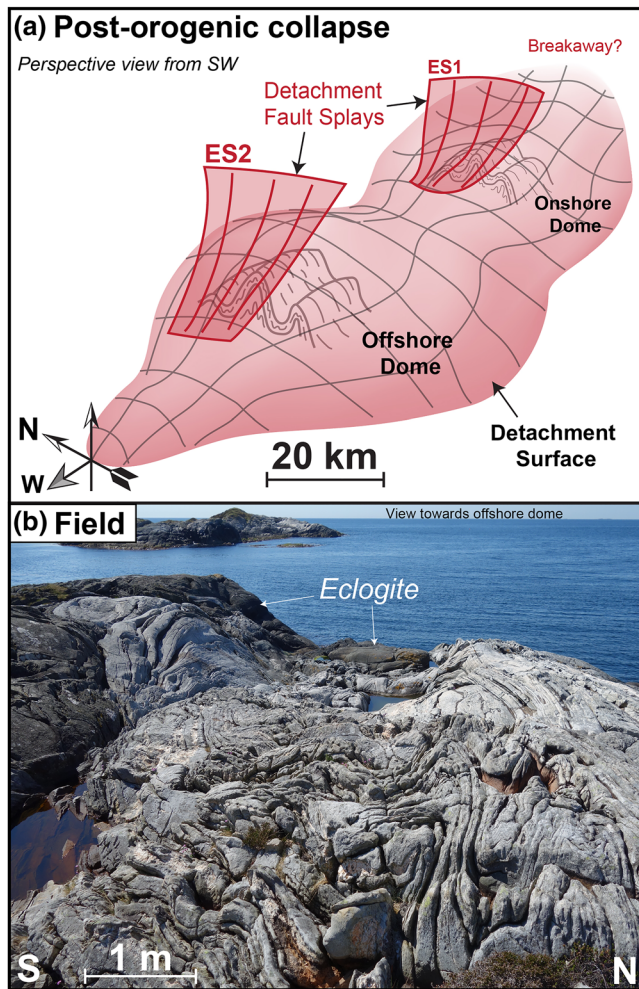
Figure 5. (a) Postorogenic collapse formed gneiss domes with upright folds and the hyperbolic geometry of the detachment, probably related to individual excisement splays (ES1 and ES2). (b) Field photo from the westernmost outcrop of the onshore dome showing folded gneisses and eclogite boudins characteristic for BU1 (see Figure 3 for location).

exposed on the westernmost islands. Our interpretation shows a rider block of Caledonian nappes occupying a synformal bend of the detachment (Figure 3d) considering that Caledonian allochthons crop out west of (structurally underneath) the Solund Devonian basin and constitute the closest outcrops (on the islands of Indrevær) to the apex of the onshore detachment (Figure 3a). Alternatively, the hanging wall could be occupied by Devonian basin fills; however, this distinction and the actual geometry of the hanging wall block is not critical to our interpretation.

The bends of the shallowly west dipping detachment zone in combination with its convex curvature in N-S direction (Figures 3b and 3c) define a hyperbolic surface consisting of two domes separated by a saddle (Figure 5a). This 3-D geometry is important, because it implies that most of the detachment consists of deeply or moderately dipping (oblique) strike-slip segments. True dip-slip segments exist only at the vertices of the corrugated surface.

5.2.3. Fault Geometries

The Horda Platform shows a series of half-grabens bound by major N-S striking listric normal faults formed during Permian-Triassic rifting (Figure 3d), which have been described in detail by previous studies (Bell et al., 2014; Fazlikhani et al., 2017; Fossen et al., 2016; Lenhart et al., 2019; Phillips et al., 2019; Whipp et al., 2014). Here, we focus on their relation to the three-dimensional dome and detachment geometry. The major rift faults have straight N-S strikes along most of the eastern margin of the northern North Sea (Figure 1). Around 61°N, however, the Vette and Øygarden Faults splay into several strongly curved segments (Bell et al., 2014). The resulting segments strike NW-SE (south of 61°N) and NE-SW (north of 61°N), coinciding with the SW and NW dipping flanks of the dome (Figure 3a). Some fault segments align with the ductile fabrics inside the offshore dome, merge into steeply dipping fabrics at strike-slip segments of the detachment (Figure 6), and show large displacements (≤5 km, Figure 3b). Where fault segments cut through the detachment into the core of the MCC, on the other hand, displacements diminish rapidly to below 100 m. At the western apex of the dome, E-W striking fault segments appear to transfer displacement from the Øygarden Fault onto a strongly curved segment of the Vette Fault (Figure 3a) that cuts through the detachment. In contrast, the eastern part of the dome is largely devoid of fault activity and shows only minor N-S striking faults with tens of meters of displacement (Figures 3a and 6b).

6. Discussion

We have identified an MCC along the coast of western Norway by combining detailed field and regional seismic observations. The MCC is ~100 km long in E-W direction and ~50 km wide in N-S direction. It occurs from up to 1,000 m above sea level (onshore) down to 10 km depth in the seismic data set (offshore). We discuss the present-day geometry of the MCC in the light of ductile flow and core complex exhumation during Devonian collapse (Figure 5) followed by brittle reactivation during North Sea rifting (Figure 6).

6.1. MCC and Detachment Formation During Caledonian Collapse

Early Devonian, postcollisional collapse of the Caledonian orogen formed the Gulen MCC (Wiest et al., 2019). Previously published and new unpublished Ar-Ar mica ages constrain MCC exhumation of ductile crust in between ~405 and 395 Ma (Chauvet & Dallmeyer, 1992; Walsh et al., 2013). The folded reflection geometries, which we observe both in SF1 and SF2, clearly witness ductile behavior in the offshore dome. Although we cannot date their absolute age, there is little doubt that the offshore ductile fabrics formed simultaneously
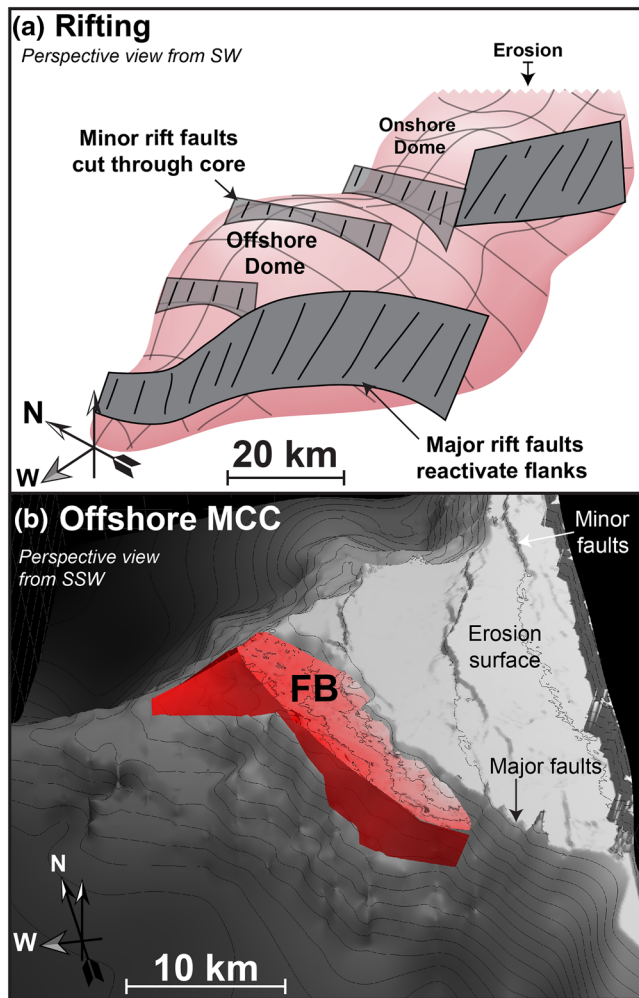
(a) Rifting
Perspective view from SW

Erosion

Onshore Dome

Minor rift faults cut through core

Offshore Dome

N

W

20 km

Major rift faults reactivate flanks

(b) Offshore MCC
Perspective view from SSW

Minor faults

Erosion surface

FB

Major faults

N

W

10 km

Figure 6. (a) During rifting, major faults reactivated the steep flanks of the offshore dome, while only minor faults cut through the core.
(b) Three-dimensional view of the MCC surface (see supporting information Figure S2 for different perspectives) resulting from brittle fault reactivation and erosion of the ductile dome. Two splays of the Øygarden Fault enclose a block of the detachment zone (red; FB).

with the onshore dome, because of (1) the striking similarity of 3-D structural geometries inside the onshore and offshore domes; (2) the continuity of the detachment zone from onshore to offshore; (3) the similar structural geometries and relationships of overlaying basement units (nappes and Devonian basins); (4) the truncation of SF2 fabrics by the top acoustic basement erosion surface.

We suggest that extension-perpendicular inward flow of deep crustal low-viscosity material formed both domes in response to upper crustal thinning during Devonian transtension (Wiest et al., 2019). The onshore and offshore domes formed in the footwall of the same large-magnitude detachment (Figure 5a), likely related to individual excisement splays (sensu Lister & Davis, 1989). Invoking a rolling hinge model for detachment formation, it seems possible that the downward stepping bends of the detachment formed sequentially related to westward migrating fault activity. Intensely strained gneisses hosting eclogite boudins witness deep crustal flow in the onshore dome (Figure 5b) and provide an analogue for the reflection geometries we observe offshore. The offshore part of this study, on the other hand, confirms the validity of structural geometries reconstructed from surface observations (Figure 3c) to a depth below 10 km (Figure 3b) and allows us to constrain the 3-D geometry of the detachment over large areas (Figure 5a).

6.2. Structural Inheritance During Rifting

Devonian collapse removed the excess gravitational potential of the over-thickened Caledonian crust (Séguret et al., 1989) and fundamentally re-equilibrated the geological and thermal structure of the continental crust in West Norway (Osmundsen et al., 2005; Souche et al., 2012; Svensen et al., 2001; Wiest et al., 2019). While the structural template remained, the thermal effect of this crustal revolution diminished in the 140 Myr in between Devonian collapse and the first North Sea rift phase, which initiated in between 261 and 236 Ma (Ter Voorde et al., 2000). Although both phases had a similar E-W extension direction (Fossen et al., 2016), Permian-Triassic rifting affected a lithosphere with very different thermal and rheological properties than Devonian collapse, resulting in fundamentally different structural styles.

6.2.1. Brittle Faults Reactivated Detachment Zone

While Devonian collapse formed MCCs, low-angle detachments and supradetachment basins, Permian-Triassic rift faults bound half-grabens (Bell et al., 2014; Whipp et al., 2014) and dissect almost the entire crust (Odinsen et al., 2000). These rift faults strike N-S over large parts of the eastern margin of the northern North Sea rift (Figure 1), but around 61°N they splay into multiple segments that align with oblique striking detachment segments (Figure 3), effectively retracing the inherited dome (Figure 6). Our onshore-offshore correlation suggests that brittle rift faults reactivated the MCC-bounding detachment, however, with highly variable effects along different segments of the detachment.

The above interpretation is supported by numerous other studies documenting brittle reactivation of previously ductile shear zones, both onshore Norway (Andersen et al., 1999; Eide et al., 1997; Ksienzyk et al., 2016; Torgersen et al., 2015; Torsvik et al., 1992), in the North Sea rift (Fazlikhani et al., 2017; Fossen et al., 2016; Lenhart et al., 2019; Osagiede et al., 2020; Phillips et al., 2019), and in other areas (e.g., Daly et al., 1989; Piqué & Laville, 1996; Salomon et al., 2015; Smith & Mosley, 1993). Our study gives new insights into the spatial variability of shear zone reactivation by brittle faults that previously could not be recognized in 2-D seismic data. Due to the complex 3-D geometry of the inherited shear zones, segments of the same fault can either merge into or cross cut the preexisting ductile fabrics. This results in large displacement variations even within small areas and induces complex fault linkage patterns.
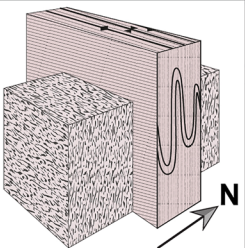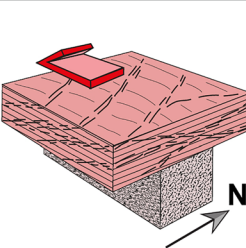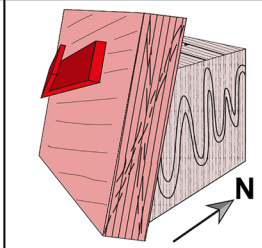
	Core SZ	Dip-slip detachment	Strike-slip detachment
Anisotropy	Strong	Very Strong	Very Strong
Shear strength	Strong	Weak	Weak
Dip	Subvertical	Subhorizontal	Steep
Strike	Parallel	Perpendicular	Oblique
Reactivation Potential	**Low**	**Moderate**	**High**

Figure 7. Schematic illustration showing three end-member types of shear zones and factors that determine their reactivation potential for brittle faults. "Strike" refers to the orientation relative to the E-W extension direction during rifting. Based on Wiest et al. (2019).

6.2.2. Brittle Reactivation of Shear Zones: Causal or Casual?

By comparing the varying reactivation styles of different types of shear zones with their contrasting characteristics mapped in the field (Figure 7), we can discuss the causality of structural inheritance.

1. Gneissic and mylonitic shear zones in the high-grade core of the MCC have strong fabric anisotropies with steeply dipping foliations, but they are mostly avoided or cut perpendicular by brittle faults. This appears mainly due to their strike parallel to the E-W extension direction of the rift. Furthermore, amphibolite facies shear zone rocks must not necessarily be particularly weak and even if, recovery during exhumation can anneal weak zones (Fossen & Cavalcante, 2017). A rift direction perpendicular to the strike of this type of shear zones can significantly increase their reactivation potential for brittle faults (Osmundsen et al., 2005). However, they may be unrecognizable in seismic data because they are vertically orientated and unlikely to be associated with large impedance contrasts.
2. The detachment zone lithologies contain large volumes of phyllosilicates, for example, nappe-derived mica schists or phyllonites formed through retrograde fluid–rock interaction (Wiest et al., 2020). Such phyllosilicate-rich rocks are associated with very low shear strength, in particular parallel to their foliation planes (Bos & Spiers, 2002; Braathen et al., 2004; Wintsch et al., 1995). Dip-slip segments of the detachment zone strike parallel to rift faults. Nevertheless, they exhibit a limited reactivation potential because of their subhorizontal orientation. Permian reactivation has been proven for some of the low-angle detachments (Eide et al., 1997; Torsvik et al., 1992), but field (Figure 4d) and seismic observations show many normal faults that cut through these subhorizontal layers even though they are weak (Fazlikhani et al., 2017; Fossen et al., 2016).
3. Strike-slip segments of the detachment on the flanks of the domes, on the other hand, combine very strong anisotropy, large volumes of weak materials, a steep dip around 60°, and an orientation oblique to the extension direction of the rift. The combination of these factors determined their high reactivation potential for brittle faults and explains why rift faults reactivated the flanks of the MCC.

6.2.3. An MCC Is More Than a Shear Zone

Both, the high-grade gneissic core and mantling detachments zones, represent previously ductile shear zones or pervasively flowing material. Yet, the two essential elements of MCCs show opposing reactivation patterns: While the gneissic core is largely spared, rift faults follow the detachment zone and thereby mold

the shape of the inherited MCC. Our above discussion highlights causal relationships between brittle reactivation and shear zone characteristics. Moreover, at large scale, the structural inheritance of an MCC with strong gneissic core and weak envelope might have caused brittle strain localization at the interface, in particular in high-angle segments on dome flanks.

The opposing role of gneiss cores and detachment zones has important implications for our understanding of areas that evolve through different modes of continental extension, similarly to the classical Basin and Range province (Buck, 1991). The gneissic core of MCCs is predestined to form long-lived structural highs during rifting, while reactivation of the detachment controls the local distribution of synrift depocenters. The gneissic cores can get exposed to the surface, become eroded and constitute sediment sources over long time periods in the development of rifts (Eide et al., 2005; Osmundsen et al., 2005). This behavior, however, relates to the structures and lithologies within the metamorphic core, which strongly depend on the crustal rheology and 3-D strain field during MCC formation. Thus, our study highlights that we need to constrain 3-D geometries and distinguish different types of shear zones, to understand the influence of previously ductile structures on rifts.

7. Summary and Conclusions

A new generation of 3-D seismic reflection data allows to correlate basement seismic facies in the northern North Sea with distinct units of a MCC mapped onshore West Norway. Our onshore-offshore correlation constrains two structurally similar domes aligned in the footwall of an ~100 km long shallowly west dipping detachment. Devonian collapse of the Caledonian orogen formed both domes and the hyperbolic detachment geometry, which comprises (oblique) strike-slip segments. Permian-Triassic rifting brittlely reactivated steep detachments on the flanks of the MCC, while rift faults cut through low-angle dip-slip segments and subvertical gneissic shear zones in the core. MCC reactivation resulted in strongly deviating fault orientations and complex fault linkage patterns. This study highlights that the notoriously three-dimensional geometry of MCCs and detachments needs to be considered to determine the brittle reactivation potential of previously ductile shear zones. Where lithospheric extension evolved from orogen collapse to rifting, inherited MCCs can locally alter the rift architecture and play a crucial role for the development of long-lived structural highs.

Data Availability Statement

Uninterpreted and interpreted seismic sections are available in the supporting information. Data sets for this research are included in Wiest et al. (2019) and Wrona et al. (2019).

References

Andersen, T. B., Osmundsen, P. T., & Jolivet, L. (1994). Deep crustal fabrics and a model for the extensional collapse of the southwest Norwegian Caledonides. *Journal of Structural Geology*, *16*(9), 1191–1203. https://doi.org/10.1016/0191-8141(94)90063-9

Andersen, T. B., Torsvik, T. H., Eide, E. A., Osmundsen, P. T., & Faleide, J. I. (1999). Permian and Mesozoic extensional faulting within the Caledonides of central south Norway. *Journal of the Geological Society*, *156*(6), 1073–1080. https://doi.org/10.1144/gsjgs.156.6.1073

Bartholomew, I. D., Peters, J. M., & Powell, C. M. (1993). Regional structural evolution of the North Sea: Oblique slip and the reactivation of basement lineaments, Geological Society, London. *Petroleum Geology Conference series*, *4*(1), 1109–1122. https://doi.org/10.1144/0041109

Bell, R. E., Jackson, C. A. L., Whipp, P. S., & Clements, B. (2014). Strain migration during multiphase extension: Observations from the northern North Sea. *Tectonics*, *33*, 1936–1963. https://doi.org/10.1002/2014tc003551

Bingen, B., Skar, O., Marker, M., Sigmond, E. M. O., Nordgulen, O., Ragnhildstveit, J., et al. (2005). Timing of continental building in the Sveconorwegian orogen, SW Scandinavia. *Norwegian Journal of Geology*, *85*(1–2), 87–116.

Bos, B., & Spiers, C. J. (2002). Frictional-viscous flow of phyllosilicate-bearing fault rock: Microphysical model and implications for crustal strength profiles. *Journal of Geophysical Research*, *107*(B2), 2028. https://doi.org/10.1029/2001JB000301

Braathen, A., Nordgulen, O., Osmundsen, P. T., Andersen, T. B., Solli, A., & Roberts, D. (2000). Devonian, orogen-parallel, opposed extension in the Central Norwegian Caledonides. *Geology*, *28*(7), 615–618. https://doi.org/10.1130/0091-7613(2000)28

Braathen, A., Osmundsen, P. T., & Gabrielsen, R. H. (2004). Dynamic development of fault rocks in a crustal-scale detachment: An example from western Norway. *Tectonics*, *23*, TC4010. https://doi.org/10.1029/2003tc001558

Brun, J.-P., Sokoutis, D., Tirel, C., Gueydan, F., Van Den Driessche, J., & Beslier, M.-O. (2018). Crustal versus mantle core complexes. *Tectonophysics*, *746*, 22–45. https://doi.org/10.1016/j.tecto.2017.09.017

Brune, S., Heine, C., Clift, P. D., & Pérez-Gussinyé, M. (2017). Rifted margin architecture and crustal rheology: Reviewing Iberia-Newfoundland, Central South Atlantic, and South China Sea. *Marine and Petroleum Geology*, *79*, 257–281. https://doi.org/10.1016/j.marpetgeo.2016.10.018

Buck, W. R. (1991). Modes of continental lithospheric extension. *Journal of Geophysical Research*, *96*(B12), 20,161–20,178. https://doi.org/10.1029/91JB01485

Chauvet, A., & Dallmeyer, R. D. (1992). ^{40}Ar/^{39}Ar mineral dates related to Devonian extension in the southwestern Scandinavian Caledonides. *Tectonophysics*, *210*(1), 155–177. https://doi.org/10.1016/0040-1951(92)90133-Q

Christiansson, P., Faleide, J. I., & Berge, A. M. (2000). Crustal structure in the northern North Sea: An integrated geophysical study. *Geological Society, London, Special Publications*, *167*(1), 15–40. https://doi.org/10.1144/gsl.Sp.2000.167.01.02

Claringbould, J. S., Bell, R. E., Jackson, C. A. L., Gawthorpe, R. L., & Odinsen, T. (2017). Pre-existing normal faults have limited control on the rift geometry of the northern North Sea. *Earth and Planetary Science Letters*, *475*, 190–206. https://doi.org/10.1016/j.epsl.2017.07.014

Clerc, C., Ringenbach, J.-C., Jolivet, L., & Ballard, J.-F. (2018). Rifted margins: Ductile deformation, boudinage, continentward-dipping normal faults and the role of the weak lower crust. *Gondwana Research*, *53*, 20–40. https://doi.org/10.1016/j.gr.2017.04.030

Corfu, F., Andersen, T., & Gasser, D. (2014). The Scandinavian Caledonides: Main features, conceptual advances and critical questions. *Geological Society, London, Special Publications*, *390*, 9–43. https://doi.org/10.1144/SP390.25

Cowie, P. A., Underhill, J. R., Behn, M. D., Lin, J., & Gill, C. E. (2005). Spatio-temporal evolution of strain accumulation derived from multi-scale observations of Late Jurassic rifting in the northern North Sea: A critical test of models for lithospheric extension. *Earth and Planetary Science Letters*, *234*(3), 401–419. https://doi.org/10.1016/j.epsl.2005.01.039

Cuthbert, S. J., Carswell, D. A., Krogh-Ravna, E. J., & Wain, A. (2000). Eclogites and eclogites in the Western Gneiss Region, Norwegian Caledonides. *Lithos*, *52*(1), 165–195. https://doi.org/10.1016/S0024-4937(99)00090-0

Daly, M. C., Chorowicz, J., & Fairhead, J. D. (1989). Rift basin evolution in Africa: The influence of reactivated steep basement shear zones. *Geological Society, London, Special Publications*, *44*(1), 309–334. https://doi.org/10.1144/gsl.Sp.1989.044.01.17

Doré, A. G., Lundin, E. R., Fichler, C., & Olesen, O. (1997). Patterns of basement structure and reactivation along the NE Atlantic margin. *Journal of the Geological Society*, *154*(1), 85–92. https://doi.org/10.1144/gsjgs.154.1.0085

Eide, E. A., Haabesland, N. E., Osmundsen, P. T., Andersen, T. B., Roberts, D., & Kendrick, M. A. (2005). Modern techniques and Old Red problems—Determining the age of continental sedimentary deposits with Ar-40/Ar-39 provenance analysis in west-central Norway. *Norwegian Journal of Geology*, *85*(1–2), 133–149.

Eide, E. A., Torsvik, T. H., & Andersen, T. B. (1997). Absolute dating of brittle fault movements: Late Permian and late Jurassic extensional fault breccias in western Norway. *Terra Nova*, *9*(3), 135–139. https://doi.org/10.1046/j.1365-3121.1997.d01-21.x

Færseth, R. B., Gabrielsen, R., & Hurich, C. (1995). Influence of basement in structuring of the North Sea basin, offshore southwest Norway. *Norwegian Journal of Geology*, *75*, 105–119.

Færseth, R. B., Knudsen, B. E., Liljedahl, T., Midbøe, P. S., & Søderstrøm, B. (1997). Oblique rifting and sequential faulting in the Jurassic development of the northern North Sea. *Journal of Structural Geology*, *19*(10), 1285–1302. https://doi.org/10.1016/S0191-8141(97)00045-X

Fazlikhani, H., Fossen, H., Gawthorpe, R. L., Faleide, J. I., & Bell, R. E. (2017). Basement structure and its influence on the structural configuration of the northern North Sea rift. *Tectonics*, *36*, 1151–1177. https://doi.org/10.1002/2017TC004514

Fossen, H. (2000). Extensional tectonics in the Caledonides: Synorogenic or postorogenic? *Tectonics*, *19*(2), 213–224. https://doi.org/10.1029/1999tc900066

Fossen, H. (2010). Extensional tectonics in the North Atlantic Caledonides: A regional view. *Geological Society, London, Special Publications*, *335*(1), 767–793. https://doi.org/10.1144/SP335.31

Fossen, H., Cavalcante, G. C., & de Almeida, R. P. (2017). Hot versus cold orogenic behavior: Comparing the Araçuaí-West Congo and the Caledonian orogens. *Tectonics*, *36*, 2159–2178. https://doi.org/10.1002/2017TC004743

Fossen, H., & Cavalcante, G. C. G. (2017). Shear zones—A review. *Earth-Science Reviews*, *171*, 434–455. https://doi.org/10.1016/j.earscirev.2017.05.002

Fossen, H., Fazlikhani, H., Faleide, J. I., Ksienzyk, A. K., & Dunlap, W. J. (2016). Post-Caledonian extension in the West Norway–northern North Sea region: The role of structural inheritance. *Geological Society, London, Special Publications*, *439*, 465–486. https://doi.org/10.1144/SP439.6

Fossen, H., Teyssier, C., & Whitney, D. L. (2013). Transtensional folding. *Journal of Structural Geology*, *56*, 89–102. https://doi.org/10.1016/j.jsg.2013.09.004

Gee, D. G., Fossen, H., Henriksen, N., & Higgins, A. K. (2008). From the early Paleozoic platforms of Baltica and Laurentia to the Caledonide orogen of Scandinavia and Greenland. *Episodes*, *31*(1), 44–51. https://doi.org/10.18814/epiiugs/2008/v31i1/007

Gordon, S. M., Whitney, D. L., Teyssier, C., & Fossen, H. (2013). U-Pb dates and trace-element geochemistry of zircon from migmatite, Western Gneiss Region, Norway: Significance for history of partial melting in continental subduction. *Lithos*, *170*, 35–53. https://doi.org/10.1016/j.lithos.2013.02.003

Griffin, W. L., & Brueckner, H. K. (1980). Caledonian Sm–Nd ages and a crustal origin for Norwegian eclogites. *Nature*, *285*(5763), 319–321. https://doi.org/10.1038/285319a0

Hacker, B. R., Andersen, T. B., Johnston, S., Kylander-Clark, A. R. C., Peterman, E. M., Walsh, E. O., & Young, D. (2010). High-temperature deformation during continental-margin subduction & exhumation: The ultrahigh-pressure Western Gneiss Region of Norway. *Tectonophysics*, *480*(1–4), 149–171. https://doi.org/10.1016/j.tecto.2009.08.012

Hacker, B. R., Andersen, T. B., Root, D. B., Mehl, L., Mattinson, J. M., & Wooden, J. L. (2003). Exhumation of high-pressure rocks beneath the Solund Basin, Western Gneiss Region of Norway. *Journal of Metamorphic Geology*, *21*(6), 613–629. https://doi.org/10.1046/j.1525-1314.2003.00468.x

Johnston, S. M., Hacker, B. R., & Andersen, T. B. (2007). Exhuming Norwegian ultrahigh-pressure rocks: Overprinting extensional structures and the role of the Nordfjord-Sogn Detachment Zone. *Tectonics*, *26*, TC5001. https://doi.org/10.1029/2005TC001933

Jolivet, L., Menant, A., Clerc, C., Sternai, P., Bellahsen, N., Leroy, S., et al. (2018). Extensional crustal tectonics and crust-mantle coupling, a view from the geological record. *Earth-Science Reviews*, *185*, 1187–1209. https://doi.org/10.1016/j.earscirev.2018.09.010

Krabbendam, M., & Dewey, J. F. (1998). Exhumation of UHP rocks by transtension in the Western Gneiss Region, Scandinavian Caledonides. *Geological Society, London, Special Publications*, *135*(1), 159–181. https://doi.org/10.1144/GSL.SP.1998.135.01.11

Ksienzyk, A. K., Dunkl, I., Jacobs, J., Fossen, H., & Kohlmann, F. (2014). From orogen to passive margin: Constraints from fission track and (U–Th)/He analyses on Mesozoic uplift and fault reactivation in SW Norway. *Geological Society, London, Special Publications*, *390*, 679–702. https://doi.org/10.1144/SP390.27

Ksienzyk, A. K., Wemmer, K., Jacobs, J., Fossen, H., Schomberg, A. C., Sussenberger, A., et al. (2016). Post-Caledonian brittle deformation in the Bergen area, West Norway: Results from K-Ar illite fault gouge dating. *Norwegian Journal of Geology*, *96*, 275–299. https://doi.org/10.17850/njg96-3-06

Labrousse, L., Jolivet, L., Agard, P., Hebert, R., & Andersen, T. B. (2002). Crustal-scale boudinage and migmatization of gneiss during their exhumation in the UHP Province of Western Norway. *Terra Nova*, *14*(4), 263–270. https://doi.org/10.1046/j.1365-3121.2002.00422.x

Labrousse, L., Jolivet, L., Andersen, T., Agard, P., Hébert, R., Maluski, H., & Schärer, U. (2004). Pressure-temperature-time deformation history of the exhumation of ultra-high pressure rocks in the Western Gneiss Region, Norway. *Geological Society of America Special Papers*, *380*, 155–183. https://doi.org/10.1130/0-8137-2380-9.155

Larsen, O., Fossen, H., Langeland, K., & Pedersen, R. B. (2003). Kinematics and timing of polyphase post-Caledonian deformation in the Bergen area, SW Norway. *Norwegian Journal of Geology*, *83*(3), 149–165.

Lenhart, A., Jackson, C. A.-L., Bell, R. E., Duffy, O. B., Gawthorpe, R. L., & Fossen, H. (2019). Structural architecture and composition of crystalline basement offshore west Norway. *Lithosphere*, *11*, 273–293. https://doi.org/10.1130/l668.1

Lister, G. S., & Davis, G. A. (1989). The origin of metamorphic core complexes and detachment faults formed during tertiary continental extension in the Northern Colorado River Region, USA. *Journal of Structural Geology*, *11*(1–2), 65–94. https://doi.org/10.1016/0191-8141(89)90036-9

Maystrenko, Y. P., Olesen, O., Ebbing, J., & Nasuti, A. (2017). Deep structure of the northern North Sea and southwestern Norway based on 3D density and magnetic modelling. *Norwegian Journal of Geology/Norsk Geologisk Forening*, *97*, 169–210. https://doi.org/10.17850/njg97-3-01

Milnes, A., Wennberg, O., Skår, Ø., & Koestler, A. (1997). Contraction, extension and timing in the South Norwegian Caledonides: The Sognefjord transect. *Geological Society, London, Special Publications*, *121*(1), 123–148. https://doi.org/10.1144/GSL.SP.1997.121.01.06

Norton, M. G. (1986). Late Caledonide Extension in Western Norway: A response to extreme crustal thickening. *Tectonics*, *5*(2), 195–204. https://doi.org/10.1029/TC005i002p00195

Odinsen, T., Christiansson, P., Gabrielsen, R. H., Faleide, J. I., & Berge, A. M. (2000). The geometries and deep structure of the northern North Sea rift system. *Geological Society, London, Special Publications*, *167*(1), 41–57. https://doi.org/10.1144/gsl.Sp.2000.167.01.03

Osagiede, E. E., Rotevatn, A., Gawthorpe, R., Kristensen, T. B., Jackson, C. A. L., & Marsh, N. (2020). Pre-existing intra-basement shear zones influence growth and geometry of non-colinear normal faults, western Utsira High–Heimdal Terrace, North Sea. *Journal of Structural Geology*, *130*, 103908. https://doi.org/10.1016/j.jsg.2019.103908

Osmundsen, P. T., & Andersen, T. B. (1994). Caledonian compressional and late-orogenic extensional deformation in the Staveneset area, Sunnfjord, Western Norway. *Journal of Structural Geology*, *16*(10), 1385–1401. https://doi.org/10.1016/0191-8141(94)90004-3

Osmundsen, P. T., & Andersen, T. B. (2001). The middle Devonian basins of western Norway: Sedimentary response to large-scale trans-tensional tectonics? *Tectonophysics*, *332*(1–2), 51–68. https://doi.org/10.1016/S0040-1951(00)00249-3

Osmundsen, P. T., Braathen, A., Sommaruga, A., Skilbrei, J. R., Nordgulen, O., Roberts, D., et al. (2005). Metamorphic core complexes and gneiss-cored culminations along the Mid-Norwegian margin: An overview and some current ideas. *Norwegian Petroleum Society Special Publications*, *12*, 29–41. https://doi.org/10.1016/S0928-8937(05)80042-6

Osmundsen, P. T., & Péron-Pinvidic, G. (2018). Crustal-scale fault interaction at rifted margins and the formation of domain-bounding breakaway complexes: Insights from offshore Norway. *Tectonics*, *37*, 935–964. https://doi.org/10.1002/2017tc004792

Peron-Pinvidic, G., Manatschal, G., & Osmundsen, P. T. (2013). Structural comparison of archetypal Atlantic rifted margins: A review of observations and concepts. *Marine and Petroleum Geology*, *43*, 21–47. https://doi.org/10.1016/j.marpetgeo.2013.02.002

Phillips, T. B., Fazlikhani, H., Gawthorpe, R. L., Fossen, H., Jackson, C. A.-L., Bell, R. E., et al. (2019). The influence of structural inheritance and multiphase extension on rift development, the northern North Sea. *Tectonics*, *38*, 4099–4126. https://doi.org/10.1029/2019tc005756

Phillips, T. B., Jackson, C. A. L., Bell, R. E., Duffy, O. B., & Fossen, H. (2016). Reactivation of intrabasement structures during rifting: A case study from offshore southern Norway. *Journal of Structural Geology*, *91*, 54–73. https://doi.org/10.1016/j.jsg.2016.08.008

Piqué, A., & Laville, E. (1996). The central Atlantic rifting: Reactivation of Palaeozoic structures? *Journal of Geodynamics*, *21*(3), 235–255. https://doi.org/10.1016/0264-3707(95)00022-4

Roberts, N. M. W., & Slagstad, T. (2015). Continental growth and reworking on the edge of the Columbia and Rodinia supercontinents; 1.86–0.9 Ga accretionary orogeny in southwest Fennoscandia. *International Geology Review*, *57*, 1582–1606. https://doi.org/10.1080/00206814.2014.958579

Røhr, T. S., Corfu, F., Austrheim, H., & Andersen, T. B. (2004). Sveconorwegian U-Pb zircon and monazite ages of granulite-facies rocks, Hisarøya, Gulen, Western Gneiss Region, Norway. *Norwegian Journal of Geology*, *84*(4), 251–256.

Salomon, E., Koehn, D., & Passchier, C. (2015). Brittle reactivation of ductile shear zones in NW Namibia in relation to South Atlantic rifting. *Tectonics*, *34*, 70–85. https://doi.org/10.1002/2014tc003728

Séguret, M., Séranne, M., Chauvet, A., & Brunel, A. (1989). Collapse basin: A new type of extensional sedimentary basin from the Devonian of Norway. *Geology*, *17*(2), 127–130. https://doi.org/10.1130/0091-7613(1989)017<0127:Cbanto>2.3.Co;2

Seranne, M., & Seguret, M. (1987). The Devonian basins of western Norway: Tectonics and kinematics of an extending crust. *Geological Society, London, Special Publications*, *28*(1), 537–548. https://doi.org/10.1144/GSL.SP.1987.028.01.35

Slagstad, T., Roberts, N. M. W., Marker, M., Rohr, T. S., & Schiellerup, H. (2013). A non-collisional, accretionary Sveconorwegian orogen. *Terra Nova*, *25*, 30–37. https://doi.org/10.1111/ter.12001

Smith, M., & Mosley, P. (1993). Crustal heterogeneity and basement influence on the development of the Kenya Rift, East Africa. *Tectonics*, *12*(2), 591–606. https://doi.org/10.1029/92tc01710

Souche, A., Beyssac, O., & Andersen, T. B. (2012). Thermal structure of supra-detachment basins: A case study of the Devonian basins of western Norway. *Journal of the Geological Society*, *169*(4), 427–434. https://doi.org/10.1144/0016-76492011-155

Stratford, W., Thybo, H., Faleide, J. I., Olesen, O., & Tryggvason, A. (2009). New Moho map for onshore southern Norway. *Geophysical Journal International*, *178*(3), 1755–1765. https://doi.org/10.1111/j.1365-246X.2009.04240.x

Svensen, H., Jamtveit, B., Banks, D. A., & Karlsen, D. (2001). Fluids and halogens at the diagenetic–metamorphic boundary: Evidence from veins in continental basins, western Norway. *Geofluids*, *1*(1), 53–70. https://doi.org/10.1046/j.1468-8123.2001.11003.x

Ter Voorde, M., Færseth, R. B., Gabrielsen, R. H., & Cloetingh, S. A. P. L. (2000). Repeated lithosphere extension in the northern Viking Graben: A coupled or a decoupled rheology? *Geological Society, London, Special Publications*, *167*(1), 59–81. https://doi.org/10.1144/gsl.Sp.2000.167.01.04

Torgersen, E., Viola, G., Zwingmann, H., & Harris, C. (2015). Structural and temporal evolution of a reactivated brittle–ductile fault—Part II: Timing of fault initiation and reactivation by K–Ar dating of synkinematic illite/muscovite. *Earth and Planetary Science Letters*, *410*, 212–224. https://doi.org/10.1016/j.epsl.2014.09.051

Torsvik, T. H., Sturt, B. A., Swensson, E., Andersen, T. B., & Dewey, J. F. (1992). Palaeomagnetic dating of fault rocks: Evidence for Permian and Mesozoic movements and brittle deformation along the extensional Dalsfjord Fault, western Norway. *Geophysical Journal International*, *109*(3), 565–580. https://doi.org/10.1111/j.1365-246X.1992.tb00118.x

Vetti, V. V., & Fossen, H. (2012). Origin of contrasting Devonian supradetachment basin types in the Scandinavian Caledonides. *Geology*, *40*(6), 571–574. https://doi.org/10.1130/G32512.1

Walsh, E. O., Hacker, B. R., Gans, P. B., Wong, M. S., & Andersen, T. B. (2013). Crustal exhumation of the Western Gneiss Region UHP terrane, Norway: ^{40}Ar/^{39}Ar thermochronology and fault-slip analysis. *Tectonophysics*, *608*, 1159–1179. https://doi.org/10.1016/j.tecto.2013.06.030

Wennberg, O. P., Milnes, A. G., & Winsvold, I. (1998). The northern Bergen Arc Shear Zone—An oblique-lateral ramp in the Devonian extensional detachment system of western Norway. *Norsk Geologisk Tidsskrift*, *78*(3), 169–184.

Whipp, P. S., Jackson, C. A. L., Gawthorpe, R. L., Dreyer, T., & Quinn, D. (2014). Normal fault array evolution above a reactivated rift fabric; a subsurface example from the northern Horda Platform. *Norwegian North Sea, Basin Research*, *26*, 523–549. https://doi.org/10.1111/bre.12050

Whitney, D. L., Teyssier, C., Rey, P., & Buck, W. R. (2013). Continental and oceanic core complexes. *Geological Society of America Bulletin*, *125*, 273–298. https://doi.org/10.1130/B30754.1

Wiest, J. D., Fossen, H., & Jacobs, J. (2020). Shear zone evolution during core complex exhumation—Implications for continental detachments. *Journal of Structural Geology*, *140*, 104139. https://doi.org/10.1016/j.jsg.2020.104139

Wiest, J. D., Jacobs, J., Ksienzyk, A. K., & Fossen, H. (2018). Sveconorwegian vs. Caledonian orogenesis in the eastern Øygarden Complex, SW Norway—Geochronology, structural constraints and tectonic implications. *Precambrian Research*, *305*, 1–18. https://doi.org/10.1016/j.precamres.2017.11.020

Wiest, J. D., Osmundsen, P. T., Jacobs, J., & Fossen, H. (2019). Deep crustal flow within post-orogenic metamorphic core complexes—Insights from the southern Western Gneiss Region of Norway. *Tectonics*, *38*, 4267–4289. https://doi.org/10.1029/2019TC005708

Wintsch, R. P., Christoffersen, R., & Kronenberg, A. K. (1995). Fluid-rock reaction weakening of fault zones. *Journal of Geophysical Research*, *107*(B2), 13,021–13,032. https://doi.org/10.1029/94JB02622

Wrona, T., Magee, C., Fossen, H., Gawthorpe, R. L., Bell, R. E., Jackson, C. A.-L., & Faleide, J. I. (2019). 3-D seismic images of an extensive igneous sill in the lower crust. *Geology*, *47*, 729–733. https://doi.org/10.1130/g46150.1

Ziegler, P. A. (1982). Triassic rifts and facies patterns in Western and Central Europe. *Geologische Rundschau*, *71*(3), 747–772. https://doi.org/10.1007/BF01821101